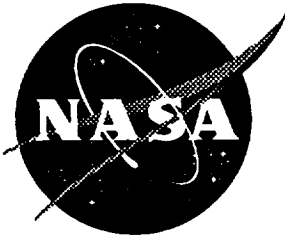


1N-36  
021538

NASA Contractor Report 201666



# MSTB 2 × 6-Inch Low Speed Tunnel Turbulence Generator Grid/Honeycomb PIV Measurements and Analysis

James L. Blackshire  
*ViGYAN, Inc., Hampton, Virginia*

Contract NAS1-19505

January 1997

National Aeronautics and  
Space Administration  
Langley Research Center  
Hampton, Virginia 23681-0001



# **MSTB 2 x 6-inch Low Speed Tunnel Turbulence Generator Grid/Honeycomb PIV Measurements and Analysis**

## **Abstract**

An assessment of the turbulence levels present in the Measurement Science and Technology (MSTB) branch's 2 x 6-inch low speed wind tunnel was made using Particle Image Velocimetry (PIV), and a turbulence generator consisting of a grid/honeycomb structure. Approximately 3000 digital PIV images were captured and analyzed covering an approximate 2 x 6-inch area along the centerline of the tunnel just beyond the turbulence generator system. Custom software for analysis and acquisition was developed for semi-automated digital PIV image acquisition and analysis. Comparisons between previously obtained LTA and LV turbulence measurements taken in the tunnel are presented.

# **MSTB 2 x 6-inch Low Speed Tunnel Turbulence Generator Grid/Honeycomb PIV Measurements and Analysis**

## **Introduction**

Particle Image Velocimetry (PIV) measurements were taken as part of the NASA Langley Advanced Subsonic Technology (AST) program to better understand the turbulence levels of the Measurement Science and Technology (MSTB) low speed wind tunnel for later use in noise reduction experiments. A grid/honeycomb structure was used to produce known turbulence levels in the tunnel for measurement/probing with the newly developed digital PIV technique. The goal was to test the feasibility of using digital PIV to make highly accurate turbulence measurements, and to assess the turbulence characteristics of the tunnel in general. A comparison of previously made LTA and LV turbulence measurements obtained in the tunnel under a similar configuration was also made.

## **Particle Image Velocimetry (PIV) System Description**

Particle Image Velocimetry is an instantaneous 2-D non-intrusive global velocimetry measurement technique that has become well established in the fluid mechanics measurement community. A basic PIV system involves taking a double exposure recording of typically  $\mu\text{m}$ -sized seed tracer particles entrained in a flow of interest.<sup>1</sup> Auto- or cross-correlation analysis techniques are then used to measure the local displacement levels of the particle image pairs, which can be used to gain access to local velocity levels in the flow given the original pulse separation timing between the double pulsed light sheets.

Beyond providing basic information about spatial distributions of velocity in a flow, ensemble statistics are often used to measure the spatially resolved mean flow, standard deviations, turbulence statistics, and velocity and vorticity correlation levels, among other things.<sup>2,3</sup> In the present application, estimates of 1st and 2nd order turbulence statistics levels were made, in addition to ensemble mean and standard deviation levels.

## **Tunnel Description and Turbulence Generator System**

The MSTB low speed wind tunnel is a small subsonic open-air induction type (Figure 1). Its test section has a cross section of 50x150mm, a length of 600mm, and a maximum velocity of 15m/s. The test section is constructed of high quality glass to provide optical access for the PIV light sheets and imaging system. The tunnel was originally designed to provide a stable and highly

laminar flow. Seed is introduced at the open inlet structure. The seed in this test was provided by a commercial TSI six jet atomizer using mineral oil with a nominal seed size of 1  $\mu\text{m}$ .

The MSTB wind tunnel had previously been tested for turbulence levels using Laser Transit Anemometry (LTA) and Laser Velocimetry (LV) techniques.<sup>4</sup> In those tests, a turbulence generator system was used based on a design similar to one used by Xia et. al.<sup>5</sup> in which various honeycomb/screen combinations were used to set up and study turbulence. The honeycomb and screen combination used in this set of tests consisted of a course screen located 200 mm upstream of a honeycomb section of length 127 mm (Figure 2). The course screen was constructed of a 1mm diameter wire mesh grid at 12.7mm<sup>2</sup> spacing, which gave an open area percentage of 80%. The honeycomb consisted of approximately 100 plastic straws cut to length (127mm), and fit snugly within the glass test cell through a removable bottom section. This configuration sets up an unsteady flow field behind the honeycomb with known turbulence levels.

### **PIV Acquisition Description**

The PIV acquisition system used for this set of tests was designed, built, and operated by S.M. Bartram and W.M. Humphreys of NASA LaRC (RTG/FMAD/MSTB). It uses two frequency-doubled Nd:YAG lasers operating at 532nm, with approximately 600mj energy levels, and 10Hz pulse repetition rates. Co-linear light sheets of approximately 1mm thickness by 100mm width were formed and directed into the test section area (Figure 3). The imaging system consisted of a custom polarizing cube image shifter system and a Kodak Megaplug 1.4 digital camera system with the camera lens system chosen to provide approximate 1:2 imaging. The entire imaging system was mounted on a precision translation stage to allow imaging different regions along the length of the test section without disturbing the light sheet or tunnel orientation. Digital images were captured and sent to an IBM compatible PC/AT 486/120 computer for storage using custom control software which is described in more detail in Appendix A.

The region and coverage areas studied in this test are depicted in Figure 4. All stations were taken along the tunnel centerline both vertically and in the transverse direction of the flow, with the initial station covering just past the honeycomb structure to approximately 19mm downstream. Each digitally captured image (1320x1035 pixels) covered a 18.86mm x 14.79mm area in the test cell. An approximate 30% overlap was provided between stations, which resulted in a translation of 13mm between each station. 14 stations were taken in all providing a total coverage area of 15.0mm by 182mm.

### **PIV Analysis/Validation Processing Description**

A custom and automated PIV analysis system was used in this effort based on a PC/AT 486/120 platform incorporating an Alacron/i860 array processing system. The system is currently

capable of processing 5 autocorrelation displacement measurements per second, and completes an entire image field in 1 minute with 50% oversampling. Details of the digital PIV analysis system algorithms developed for this effort are provided in Appendix A. A 128x128 pixel correlation size was used to provide the needed accuracy levels. This translates to an approximate 1.829mm spatial resolution capability, and a 0.914mm measurement resolution size. Image sizes ranged from 15-50  $\mu\text{m}$  which covered 3-8 pixels on the digital camera. This, along with seed density levels of 3-20 image pairs per  $\text{mm}^2$ , resulted in correlation signals with SNR of approximately 50:1. A weighted mean centroiding scheme was used, and provided measurement sensitivity levels of 0.1 to 0.8 pixels, which corresponds to a lower limit of approximately 2 to 10  $\mu\text{m}$ . A typical autocorrelation processing step is depicted in Figure 5, which shows a raw 128x128 pixel digital image area, its autocorrelation pattern, and the resulting scaled vector output.

An assessment of the image shift calibration stability of the system was made, the results of which are depicted in Figure 6. Station-to-station image shift variations were noticed in both the axial and transverse component levels, and were most likely due to minor variations in the relative mirror alignment of the image shifter due to mechanical vibration or temperature fluctuation levels present during the test. An increase in the axial image shift level and decrease in the transverse image shift level of +66.89  $\mu\text{m}$  and -98.8  $\mu\text{m}$  were noticed, respectively, from station 1 to station 14, with ensemble station standard deviation levels present of 15-29  $\mu\text{m}$ .

Data validation and post processing efforts also involved using custom and automated algorithms based on a PC/AT 486/120 computer platform. Measurement validation rates ranged from 10-60% percent based primarily upon the image quality and seed levels available in the raw data. A four-tiered validation routine was used to reduce the analyzed data. This involved a bandpass validator operation, followed by a local median validator, a 3x3 local mean filter, and finally an image shift subtraction operation. The validation process was automated, relying only minimally on operator input, and took approximately 1 second per analyzed data file. Following data validation, the ensemble mean/standard deviation, and data convergence algorithms were applied to the various data sets.

## Results

More than 3000 digital images were captured and analyzed for this test. This consisted of 200 data images and 10 image shift reference images at each of the 14 stations. The resulting ensemble averaged mean velocity field near the exit of the honeycomb structure is shown in Figure 7. Each straw in the honeycomb structure acted like a small jet which resulted in three expanding jet structures in the vector field shown in the figure. An entire straw/jet structure can be seen along the measurement centerline with 2 additional jet structures partially visible on the top and bottom of the field respectively. Data convergence for this initial measurement station is

shown in Figure 8 for nine positions in the field, corresponding to the center vector position, and 8 neighboring vector positions at 5mm vertically and horizontally displaced positions away from the center. The ensemble mean is seen to converge in a reasonable fashion with an ensemble number above 100-150 data points. The ensemble mean velocity field patterns for all stations are depicted in Figures 9 (axial component contour plot underlay) and 10 (transverse component contour plot underlay). Ensemble variance levels are depicted in Figures 11 and 13, for the axial and transverse components, respectively. Three axial cuts were taken along the length of the data set as shown in Figures 11 and 13, representing data along the center jet centerline and the jet edges between the three jets. These results are depicted in Figures 12 and 14, for the axial and transverse components, respectively.

First and second order turbulence statistics calculations were also determined for the entire data ensemble. Turbulence intensities for the  $\langle u'u' \rangle$  axial component and  $\langle v'v' \rangle$  transverse component are depicted in Figures 15 and 17. Three axial cuts were taken along the length of both of these data sets and are shown in Figures 16 and 18, respectively. Reynold's Stress and out-of-plane mean vorticity calculations were also made, and are depicted in Figures 19 and 20, respectively. Turbulence intensity and Reynold's Stress levels are seen to increase sharply just beyond the honeycomb structure, peaking at approximately 20mm downstream, and then decreasing gradually to a minimum level at 100 mm. Similar trends can be seen in the ensemble variance plots in Figures 12 and 14. Vorticity levels and trends show jet-like structures out to approximately 25 mm, with vorticity levels minimizing and stabilizing beyond that.

Standard deviation comparison plots with previously taken Laser Velocimetry (LV) and Laser Transit Anemometry (LTA) data<sup>4</sup> are depicted in Figures 21 and 22. The LV and LTA data was taken in the same MSTB wind tunnel under similar conditions. Good agreement is seen between the different techniques beyond 25 to 30 mm downstream. The PIV data, however, showed somewhat higher levels closer to the honeycomb structure. This is most likely due to the fact that PIV is a global velocimetry technique and LV and LTA are point measurement techniques. As seen in the mean velocity and standard deviation plots of Figures 9, 10, 11, and 13, the levels are seen to vary considerably in the jet structure regions. The likelihood that the PIV axial cut position along the jet edge, and the LTA and LV point measurement locations in the transverse directions were coincident, is not very good. General trends and standard deviation levels are in good agreement between the three techniques, however.

## Summary

An assessment of the turbulence levels present in the Measurement Science and Technology (MSTB) branch's 2 x 6-inch low speed wind tunnel was made using Particle Image Velocimetry (PIV), and a turbulence generator consisting of a grid/honeycomb structure.

Approximately 3000 digital PIV images were captured and analyzed covering an approximate 2 x 6-inch area along the centerline of the tunnel just beyond the turbulence generator system. Custom software for analysis and acquisition was developed for semi-automated digital PIV image acquisition and analysis. Comparisons between previously obtained LTA and LV turbulence measurements taken in the tunnel are presented.

## Appendix A

Two software packages were developed for this effort. These included a digital PIV (DPIV) acquisition program and digital PIV analysis program for use with a Kodak Megaplug v1.4 digital camera system. The software runs under Windows 3.1 or Windows 95, and is automated with the exception of user input to a configuration file for setup parameters for each program. The input configuration files are updated with a text editor and the various parameters are read in during program execution.

The DPIV acquisition configuration file is called **DPIVWRT.CFG** and takes the form shown below:

software_version_number	1.2
Kodak_exposure_level(ms)	90
output_datafile_base_name	data1
number_of_files	100

The configuration file requires three inputs; 1) the Kodak Megaplug exposure level, 2) the output datafile base name, and 3) and the number of digital files to capture and store away. The base name is used for all the output files with the extension increasing from \*.000, \*.001, \*.002, ... to the maximum files to be saved away.

The DPIV acquisition executable file is called **DPIVWRT.EXE** and involves 5 basic steps (actual code excerpts are shown in italics):

- 1) Read in configuration file information:

```
read_config(); /* call read_config(); function call */
```

- 2) Initialize the Epix frame grabber and Kodak camera:

```
if (do_open() < 0) /* initialize framegrabber and return error if problem */  
return(1);  
pxd_videkset('h'); /* set Kodak camera system to high resolution mode */  
pxd_videkdo(7,0,exposure); /* capture initializing digital image */  
pxd_video('s', pxd_imbuf()); /* turn frame grabber display off for faster implementation */
```

- 3) Setup output data file name and begin main loop:

```
printf("\nDigitizing/writing file number: \n\n"); /* show what file number we are currently saving */
```



```
for (q = 0; q < filemax ; q++)    /* loop through the number of files */
{
```

4) Capture 1320x1035 pixel digital image:

```
pxd_videkdo(7,0,exposure);    /* capture the digital image to framegrabber */
pxd_imbuf('s', pxd_imbuf());    /* turn display off for faster implementation */
```

```
onetenhund();    /* set up the string for the output filename */
strcpy(filename, "");
strcat(filename, base);
strcat(filename, ".");
strcat(filename, filenum2);
```

```
ofp = fopen(filename, "ab");    /* get the current filename ready to write */
```

5) Read digital image from framegrabber memory and write to PC memory and then to output file:

```
for (j = 0; j < 1035; j++)    /* loop through the pixel rows one at a time */
{
    yposb = j;    /* keep track of current row position */
    ypose = j + 1;
    pxd_iopen(0, pxd_imbuf(), 0, yposb, 1320, ypose, 'r');    /* setup pixel row */
    pxd_io(0, list, 1320);    /* read pixel row */
    fwrite( list, sizeof( unsigned char ), 1320, ofp );    /* write pixel row to file */
}
fclose(ofp);    /* close file when done */
}
```

The data is written in binary form to file in row format at about 7 seconds per 1320x1035 8-bit pixel file.

The DPIV autocorrelation analysis configuration file is called **DPIVCOR.CFG** and takes the form shown below:

software_version_number	1.0
image_threshold_level(0.9-1.1)	1.0
FP_DC_peak_extent(1-20)	6
search_box_xmin(0-128)	45
search_box_xmax(0-128)	110
search_box_ymin(0-128)	25
search_box_ymax(0-128)	45
Default_peak_xpos(0-64)	2
Default_peak_ypos(0-64)	2
Centroid_threshold_level(0-255)	250
pixel_scale_factor(microns/pixel)	1.0
acquisition_magnification	1.0
laser_pulse_separation(microsec)	1.0
input_DPIV_binary_filename	data1
output_vector_datafile_name	analyz1
number_of_files_to_analyze	10

The input configuration file supplied various analysis system parameters needed for processing. These included 1) the acquisition magnification factor, 2) image and centroid threshold levels, 3) the DC peak correlation extent, 4) correlation search box limits, 5) default peak correlation pixels, 6) laser pulse separation timing, and 7) the input and output file base names and number of files to analyze.

The DPIV autocorrelation analysis executable file is called **DPIVCOR.EXE** and involves 7 basic steps (actual code excerpts are shown in italics):

- 1) Read in configuration file information:  

```
read_config();
```

*/\* call read\_config(); function call \*/*
- 2) Initialize Alacron i860 array processor:  

```
if (alopen (DEV) != 0) /* initialize i860 and check for error */
    errexit ("can't open device %d\n", DEV);
aldev (0);
if (almapload (I860PROGRAM, STACKSIZE) != 0) /* load analysis program into i860 memory */
    errexit ("can't load %s\n", I860PROGRAM);
```
- 3) Setup output data file name and begin main loop:  

```
printf("\n\n Analyzing file number:\n\n");
for (qcount = 0; qcount < filemax ; qcount++) /* loop through the number of files */
{
    onetenhund(); /* set up the strings for the output filename */
    strcpy(filename,""); /* and input filename */
    strcat(filename,base);
    strcat(filename,".");
    strcat(filename,filenum2);
    strcpy(filename2,"");
    strcat(filename2,base2);
    strcat(filename2,".");
    strcat(filename2,filenum2);
    ifp = fopen(filename, "rb");
```
- 4) Read data from file and send to PC memory and to i860 memory:  

```
read_array(); /* read data from file */
alsetba (VtoP (A_buf1), (unsigned char *)buf0, 32000); /* send data from PC */
alcall (aladdr ("_senddata"), 11, A_buf1, A_buf2, A_buf3, /* memory to i860 */
        A_buf4, A_buf5, A_buf6, A_buf7, A_buf8, A_buf9, /* memory */
        A_buf10, 1);
await 0; /* wait for completion */
```
- 5) Perform FFT and autocorrelation calculations on i860:  

```
alcall (aladdr ("_doffinew"), 2, A_buf128, A_countp); /* Run the autocorrelation routine */
await 0; /* wait for completion */
```
- 6) Perform centroid calculation:  

```
main_search(); /* Run the centroid extraction routine */
```
- 7) Write data to file:  

```
fl = fopen(ftest, "a"); /* set up output filename to write */
for (i=0; i<15; i++) /* loop for 15x19 vector array */
{
```

```

for (j=0;j<19;j++)
{
    x[k] = (x[k]*t10)/(t11*t12);    /* scale the vectors */
    x1[k] = (x1[k]*t10)/(t11*t12);
    x2[k] = (x2[k]*t10)/(t11*t12);
    y[k] = (y[k]*t10)/(t11*t12);
    y1[k] = (y1[k]*t10)/(t11*t12);
    y2[k] = (y2[k]*t10)/(t11*t12);
    count0 = ((j*1.0)+ct[0]);        /* keep track of position */
    count1 = ((i*1.0)+ct[1]);
    absx = count0;
    absy = count1;
    fprintf(fl,"%f%f%f%f%f%f%f%f%f%f%f%f%f%f%f%f", /* write to file */
        count0,count1, x[k],y[k],b[k],x1[k],
        y1[k],b1[k],x2[k],y2[k],b2[k]);

    k++;
    l--;
}
fclose(fl);                          /* close output file */

```

The data is written in ASCII format with the top three autocorrelation centroids being saved according to peak intensity level which is also saved. A weighted mean centroiding scheme is used for sub-pixel centroid extraction. The current autocorrelation algorithm running on the i860 computes 5 vectors per second which saves away the 15x19 vector array for a single file in approximately 1 minute.

## Acknowledgments

The author wishes to thank W.M. Humphreys and S.M. Bartram of the Measurement Science and Technology Branch for providing DPIV images, and for assistance and guidance in development of the various algorithms used in this effort. Thanks are also extended to Cadet Andrea Houk of the Air Force Academy for assistance in data acquisition efforts.

## References

- [1] Adriane, R. J., "Scattering Particle Characteristics and Their Effect on Pulsed Laser Measurements of Fluid Flow: Speckle Velocimetry vs Particle Image Velocimetry," Appl. Opt. 23, 1690 (1984).
- [2] Liu, Z., Landreth, C.C., Adriane, R.J., and Hanratty, T.J., "High Resolution Measurements of Turbulent Structure in a Channel with Particle Image Velocimetry," Exp. Fluids, 10, 1991, 301-312.
- [3] Yao, C., and Paschal K., "PIV Measurements of Airfoil Wake-Flow Turbulence Statistics and Turbulent Structures," 32nd Aerospace Sciences Meeting and Exhibit, Reno, NV, January 10-13, 1994.

- [4] Humphreys, W.M., and Gartrell, L.R., "Comparison of Laser Transit Anemometry Data Analysis Techniques," 14th International Congress on Instrumentation in Aerospace Simulation Facilities, Rockville, Maryland, October 27-31, 1991.
- [5] Xia, L., Farrell, C., and Kavanagh, P., "Experimental Investigation of the Unsteady Flow Behind Screens and Honeycombs," ISA Paper Number 90-143, 1990.
- [6] Humphreys, W.M., Bartram, S.M., and Blackshire, J.L., "A Survey of Particle Image Velocimetry Applications in Langley Aerospace Facilities," *31st Aerospace Sciences Meeting & Exhibit*, AIAA 93-0411, Reno, NV, January 1.

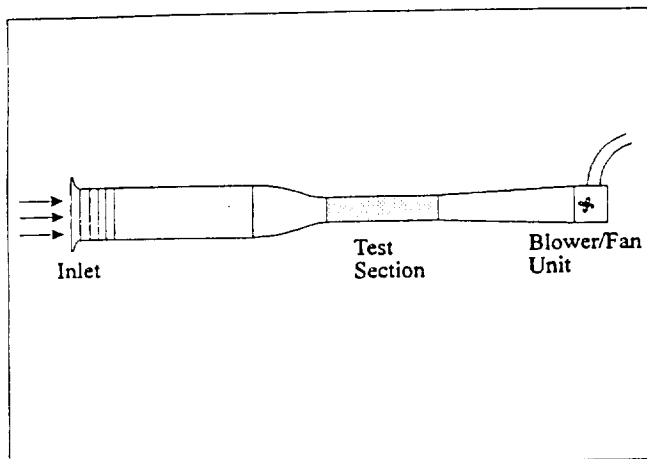


Figure 1. MSTB low speed wind tunnel.

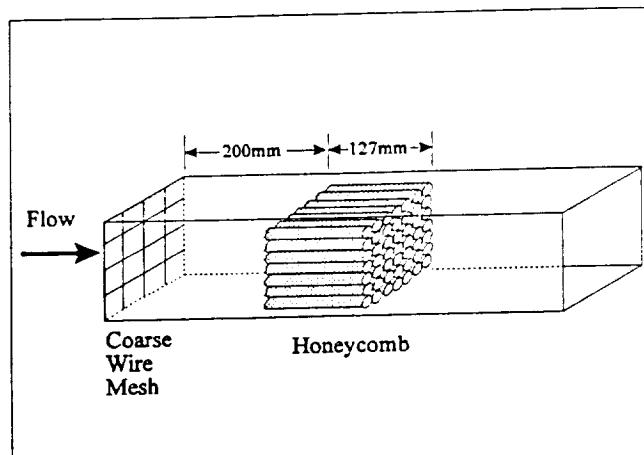


Figure 2. Turbulence generator unit.

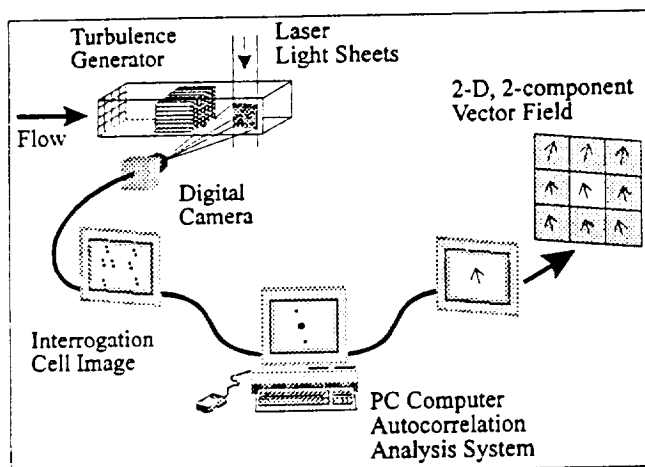


Figure 3. MSTB Particle Image Velocimetry acquisition system.

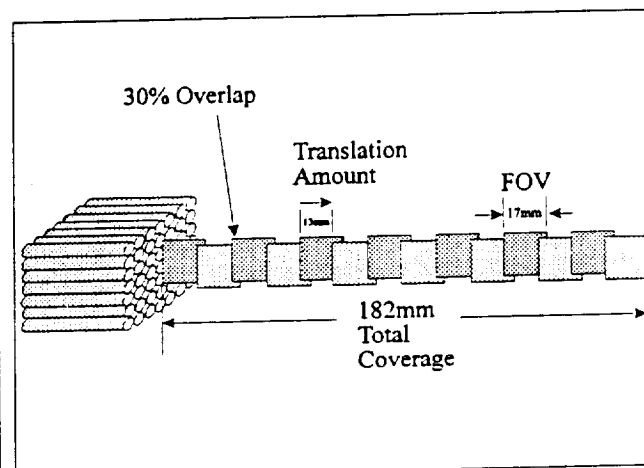


Figure 4. Measurement locations and Field of View (FOV).

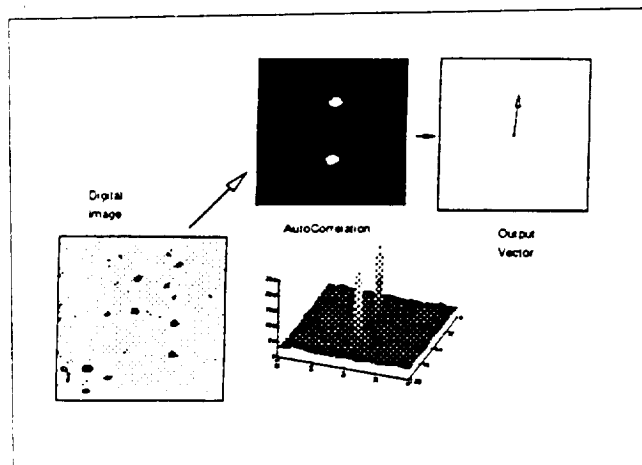


Figure 5. PIV Autocorrelation analysis processing.

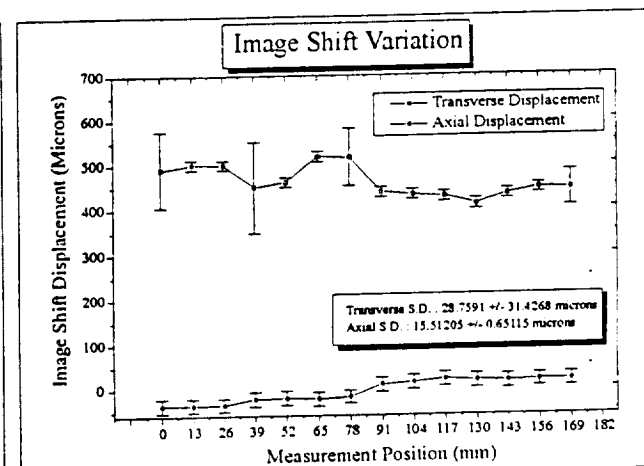


Figure 6. Image Shift fluctuation study results.

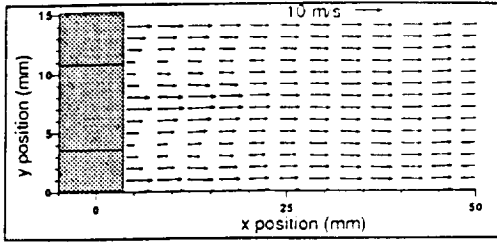


Figure 7. Ensemble mean velocity station #1.

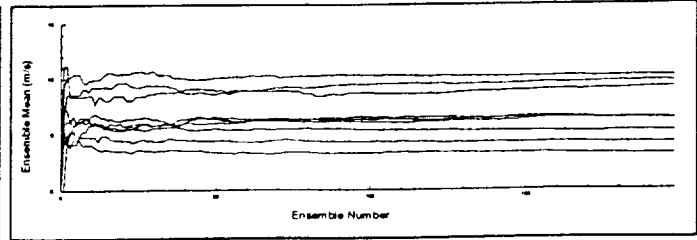


Figure 8. Ensemble mean velocity convergence for 200 files and station #1.

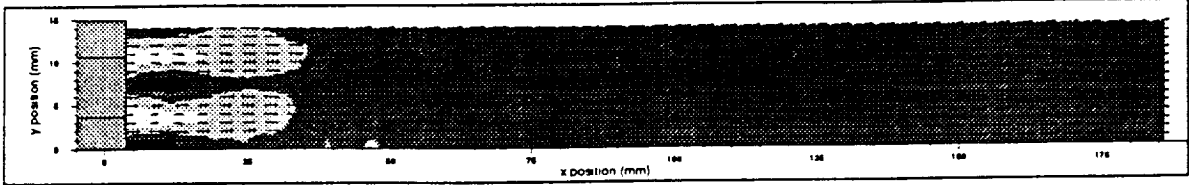


Figure 9. Ensemble mean velocity all stations with axial component contours.

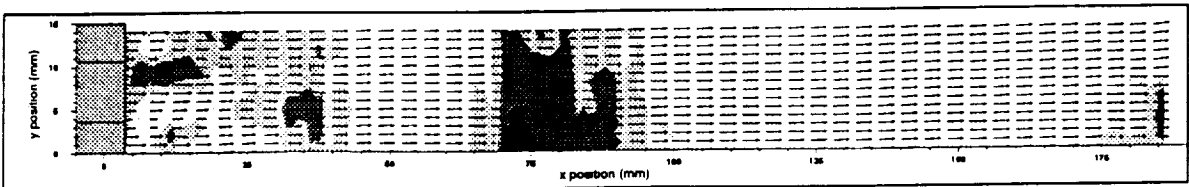


Figure 10. Ensemble mean velocity all stations with transverse component contours.

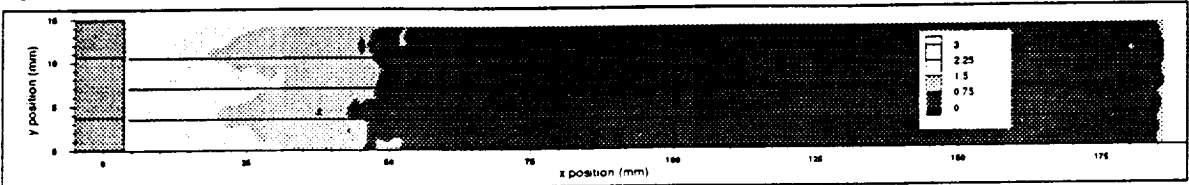


Figure 11. Ensemble axial velocity variance all stations.

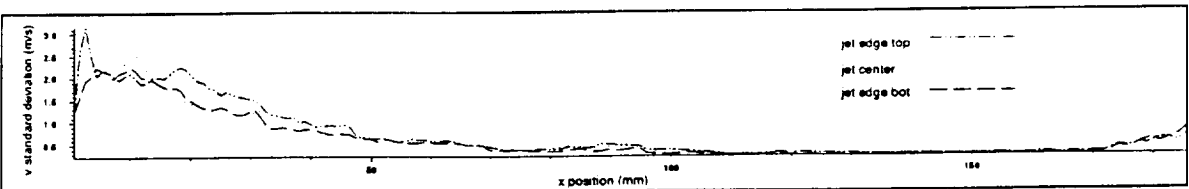


Figure 12. Axial cuts of ensemble axial velocity variance along jet centerline and jet edges.

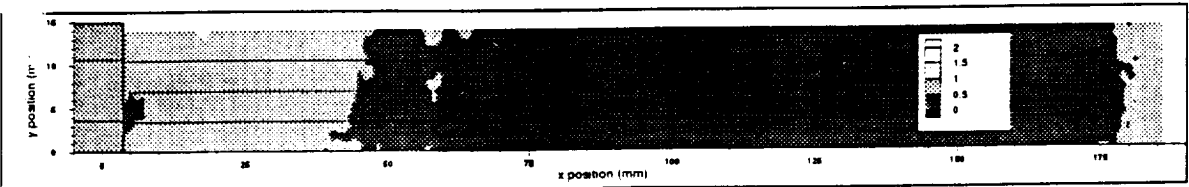


Figure 13. Ensemble transverse velocity variance all stations.

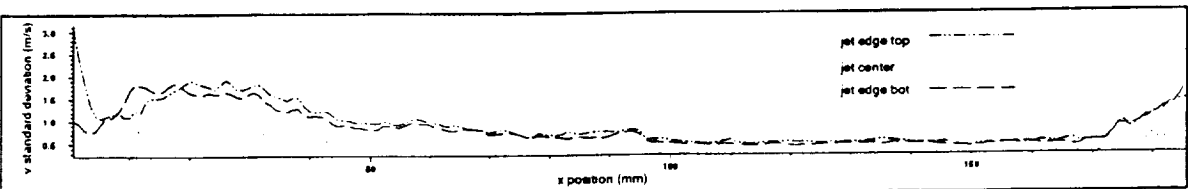


Figure 14. Axial cuts of ensemble transverse velocity variance along jet centerline and jet edges.

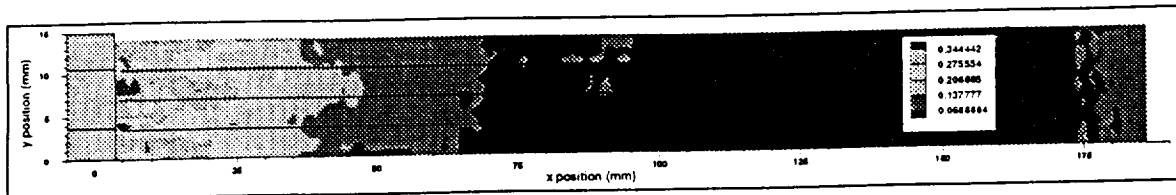


Figure 15. Turbulence Intensity  $\langle u'u' \rangle$ .

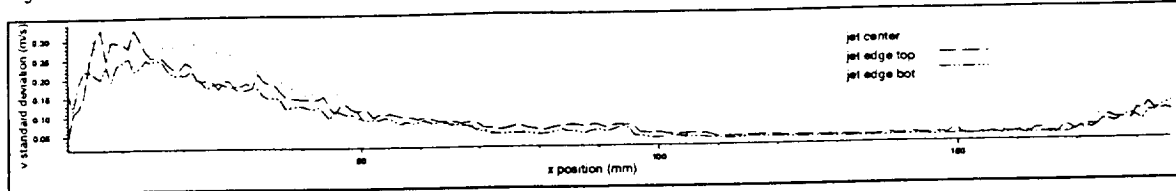


Figure 16. Axial cuts of Turbulence Intensity  $\langle u'u' \rangle$  in Figure 15.

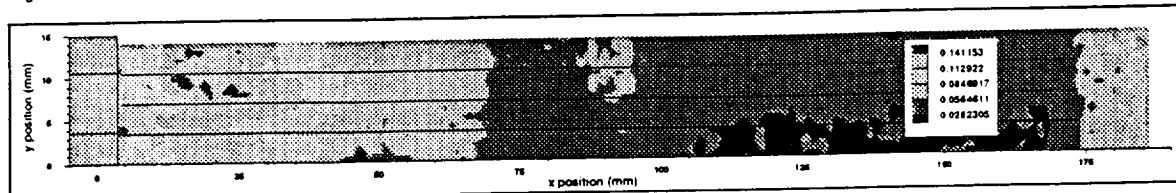


Figure 17. Turbulence Intensity  $\langle v'v' \rangle$ .

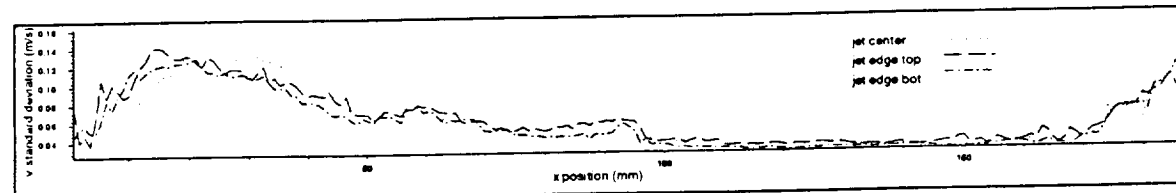


Figure 18. Axial cuts of Turbulence Intensity  $\langle v'v' \rangle$  in Figure 17.

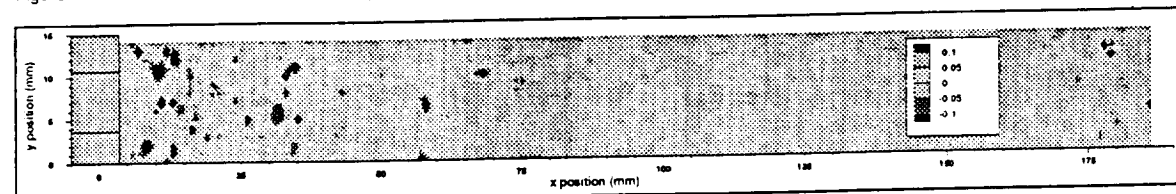


Figure 19. Reynold's Stress  $\langle u'v' \rangle$ .

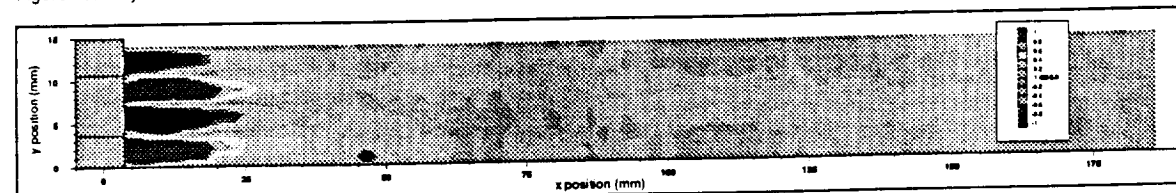


Figure 20. Out-of-plane mean vorticity.

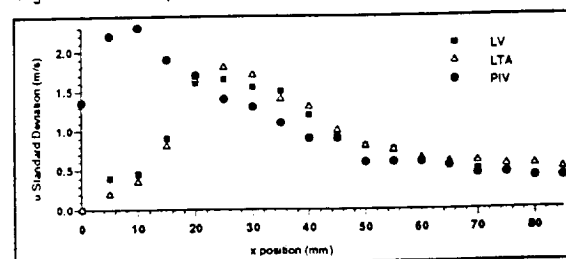


Figure 21. LV, LTA and PIV u-component Standard Deviation comparison along jet edge in axial direction.

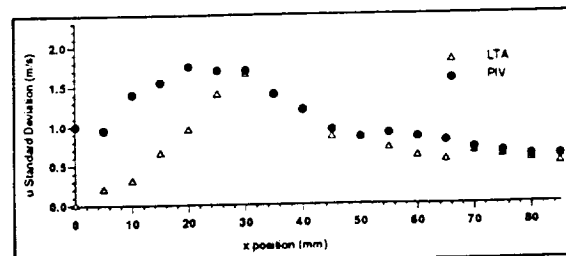


Figure 22. LTA and PIV v-component Standard Deviation comparison along jet edge in axial direction.

REPORT DOCUMENTATION PAGE			Form Approved OMB No. 0704-0188	
<small>Public reporting burden for this collection of information is estimated to average 1 hour per response, including the time for reviewing instructions, searching existing data sources, gathering and maintaining the data needed, and completing and reviewing the collection of information. Send comments regarding this burden estimate or any other aspect of this collection of information, including suggestions for reducing this burden, to Washington Headquarters Services, Directorate for Information Operations and Reports, 1215 Jefferson Davis Highway, Suite 1204, Arlington, VA 22202-4302, and to the Office of Management and Budget, Paperwork Reduction Project (0704-0188), Washington, DC 20503.</small>				
1. AGENCY USE ONLY (Leave blank)		2. REPORT DATE January 1997		3. REPORT TYPE AND DATES COVERED Contractor Report
4. TITLE AND SUBTITLE MSTB 2 x 6-inch Low Speed Tunnel Turbulence Generator Grid/Honeycomb PIV Measurements and Analysis			5. FUNDING NUMBERS C NASI - 19505 WU 538-03-12-04	
6. AUTHOR(S) James L. Blackshire				
7. PERFORMING ORGANIZATION NAME(S) AND ADDRESS(ES) Vigyan, Inc. 30 Research Dr. Hampton, Va 23666			8. PERFORMING ORGANIZATION REPORT NUMBER	
9. SPONSORING/MONITORING AGENCY NAME(S) AND ADDRESS(ES) National Aeronautics and Space Administration Langley Research Center Hampton, Va 23681-0001			10. SPONSORING/MONITORING AGENCY REPORT NUMBER NASA CR-201666	
11. SUPPLEMENTARY NOTES Langley Technical Monitor : Richard R. Antcliff Final Report				
12a. DISTRIBUTION/AVAILABILITY STATEMENT Unclassified - Unlimited Subject Category 36			12b. DISTRIBUTION CODE	
13. ABSTRACT (Maximum 200 words)  An assessment of the turbulence levels present in the Measurement Science and Technology (MSTB) branch's 2 x 6-inch low speed wind tunnel was made using Particle Image Velocimetry (PIV), and a turbulence generator consisting of a grid/honeycomb structure. Approximately 3000 digital PIV images were captured and analyzed covering an approximate 2 x 6-inch area along the centerline of the tunnel just beyond the turbulence generator system. Custom software for analysis and acquisition was developed for semi-automated digital PIV image acquisition and analysis. Comparisons between previously obtained LTA and LV turbulence measurements taken in the tunnel are presented.				
14. SUBJECT TERMS Particle Image Velocimetry, Turbulence Generator, Laser Transit Velocimetry, Laser Velocimetry			15. NUMBER OF PAGES 14	
			16. PRICE CODE A03	
17. SECURITY CLASSIFICATION OF REPORT Unclassified	18. SECURITY CLASSIFICATION OF THIS PAGE Unclassified	19. SECURITY CLASSIFICATION OF ABSTRACT	20. LIMITATION OF ABSTRACT	